Global Journal of Researches in Engineering: J General Engineering
Volume 23 Issue 4 Version 1.0 Year 2023
Type: Double Blind Peer Reviewed International Research Journal
Publisher: Global Journals
Online ISSN: 2249-4596 & Print ISSN: 0975-5861

Effect of Interlayer Thickness on Mechanical Properties of Steel/Polymer/Steel Laminates Fabricated by Roll Bonding Technique

By Payam Maleki, Abbas Akbarzadeh & Mahdi Damghani

University of the West of England (UWE)

Abstract- Nowadays, metal/polymer/metal laminates are extensively used in various industries due to their unparalleled properties. In this study, the roll bonding process was employed for lamination of low carbon steel (St14) and semi-melted thermoplastic polyurethane sheets. The T-peel and Single Lap Shear (SLS) tests were conducted to determine the optimal rolling speed to achieve the highest bond strength between the polymer core and the steel skins. Then, with the goal of investigation of the effect of polymer volume fraction on the mechanical properties of laminates, the lamination process was performed at the optimal rolling speed and various thickness reductions. The uniaxial tensile tests were conducted at three directions of 0°, 45°, and 90° with respect to rolling direction for the skin sheet and four different laminates. The results of both T-peel and SLS tests recommend the lowest rolling speed (25 rpm) to acquire maximum bond strength. The results of tensile tests show that the mechanical properties of the laminates depend on the sample direction.

Keywords: metal/polymer/metal laminate sheet, roll bonding, thermoplastic polyurethane, low carbon steel sheet, mechanical properties.

GJRE-J Classification: LCC: TA401-492

Strictly as per the compliance and regulations of:

Effect of Interlayer Thickness on Mechanical Properties of Steel/Polymer/Steel Laminates Fabricated by Roll Bonding Technique

Payam Maleki [α], Abbas Akbarzadeh [σ] & Mahdi Damghani [ρ]

Abstract- Nowadays, metal/polymer/metal laminates are extensively used in various industries due to their unparalleled properties. In this study, the roll bonding process was employed for lamination of low carbon steel (St14) and semi-melted thermoplastic polyurethane sheets. The T-peel and Single Lap Shear (SLS) tests were conducted to determine the optimal rolling speed to achieve the highest bond strength between the polymer core and the steel skins. Then, with the goal of investigation of the effect of polymer volume fraction on the mechanical properties of laminates, the lamination process was performed at the optimal rolling speed and various thickness reductions. The uniaxial tensile tests were conducted at three directions of 0°, 45°, and 90° with respect to rolling direction for the skin sheet and four different laminates. The results of both T-peel and SLS tests recommend the lowest rolling speed (25 rpm) to acquire maximum bond strength. The results of tensile tests show that the mechanical properties of the laminates depend on the sample direction. It is also observed that as the volume fraction of the polymer in the laminate structure increases, the yield strength, tensile strength and elastic modulus decrease. The bond strength of the metal/ polymer interface is directly related to the ductility behavior of the laminates.

Keywords: metal/polymer/metal laminate sheet, roll bonding, thermoplastic polyurethane, low carbon steel sheet, mechanical properties.

I. Introduction

In recent years, there has been growing research in developing materials that are lightweight and have enhanced mechanical properties compared to traditional and conventional metallic structures such as aluminum, steel, titanium, etc. During the past decades, the widespread use of traditional metallic structures has led to an abundance of readily available design data supported by extensive and expensive experimental testing that makes designing and analyzing such structures safe and more convenient. For instance, the use of aluminum alloys for more than 70 years in the manufacture of aerostructures has led to a plethora of both available design data and past experiences. This makes it convenient and safe for designers and structural analysts to use such materials in the design of aerostructures. Furthermore, the use of optimization techniques, i.e. topology, topography and size optimizations, has enabled structural designers and analysts to make metallic structures more lightweight. The use of modern manufacturing techniques such as Additive Layer Manufacturing (ALM) for metals has also contributed to making components that are lightweight. Whilst these approaches in design and manufacture are valid for single purpose structures, i.e. to be load bearing only, they are not suitable for when the structure has to be multi-functional. For instance, the metallic structures may exhibit desirable structural stiffness and strength but are not well suited for applications where high comparable specific stiffness and strength, improved isolation, superior vibration and sound damping properties and improved ductility are required [1]. Hence, scientists have resorted to alternative material systems and manufacturing methods. Amongst such material systems, hybridization has the potential to provide an economical mean [2], [3] to create material systems that can combine the advantages of miscellaneous materials, i.e. low density, high bending resistance, energy absorption, high load-capacity at low weight and etc., with each other and yield a material system that exploits the advantage of each constituent material meeting the required functions of a structure.

Amongst hybrid structures, three-layered metal/polymer/metal or multi-layer sheets, offer a great potential for the automotive, construction, naval industries and aerostructures. For instance, GLARE, a combination of aluminum layers and a Glass Fiber Reinforced Polymer (GFRP) has been applied in the construction of Airbus A380 double decker aircraft [1]. Another example is the use of Aramid Reinforced ALuminum Laminate (ARALL) for a damage tolerant wing design particularly areas prone to the fatigue loading [4]. It is worth noting that for newly adapted lightweight material systems, such as hybrid structures of metals-polymers, future gains are obtained with respect to environmental protection and sustainability. Metal/polymer/metal laminates as hybrid materials are also an alternative to homogeneous metal sheets that have polymeric properties as well as metallic characteristics. Good formability, excellent mechanical properties, lightweight, and acoustic and vibration

Author α σ: Department of Materials Science and Engineering, Sharif University of Technology, Tehran, Iran.
Author ρ: Department of Engineering, Design and Mathematics (EDM), University of the West of England (UWE), Bristol, UK.
e-mail: mahdi.damghani@uwe.ac.uk

damping are the three-layer sheets characteristics. The usage of these sheets is common in various industries.

Three-layered examples of metal/polymer/metal composites such as HYLITE have been used in automotive industry, due to their high mechanical and formability properties and being lightweight [5]. HYLITE is an aluminum/polypropylene/aluminum with thicknesses $0.2/0.8/0.2mm$ which was used in the construction of Audi A2. Another example is the use of BONDAL, a steel/polypropylene/steel composite known as steel counterpart to HYLITE, with a polymer core having approximate thickness of 50 μm. BONDAL has layer thicknesses of $0.5/0.5/0.5\,mm$ and is used for damping applications such as reducing radiating construction noise. It is worth noting that such composite material systems are being used in the aerospace industry as a result of their excellent compressive strength, high corrosion resistance, high toughness and workability. Furthermore, these sheets are currently being used in home appliances such as dishwashers and lawnmowers, where vibration and sound damping are crucial. Depending on the application of three-layer sandwich sheets in the industry, the ratio of the metal skin thickness to the polymer core, the type of metal and polymer, and the manufacturing and bonding of three-layer sheets are different.

Kim et al. [6] classified metal/polymer/metal three-layer laminates into three categories:

- Laminates with low-density polymeric core, containing 40% to 60% of the total thickness (lightweight).
- Laminates with thin polymeric core, containing 20% of the total thickness (acoustic damper).
- Laminates with very thin polymeric core (or without core) where the thickness and nature of the skins can be different (to take advantage of the different properties of both layers).

The three-layer composites metal skins mostly consist of steel sheets (often stainless steel) [7] or aluminum alloys such as AA5052 [8], AA5754 [9], and AA5182 [10] with different thicknesses. The most important criteria for selecting steel and aluminum sheets are high mechanical and formability properties [11], flexural stiffness, corrosion resistance, joinability, dent resistance, [12] and cost reduction [13]. Considering the superior inherent formability of the steel compared to aluminum, three-layer steel/polymer/steel sheets offer a higher stiffness-to-weight ratio than aluminum and steel monolithic sheets. In the assortment made by Hayashi et al. [14], specifically for laminated steel sheets, these laminates are divided into two categories; (i) vibration-damping sheets, i.e. with thickness composition of core $= 0.03\,mm - 0.1\,mm$ and skin $= 0.15\,mm - 1.6\,mm$, and (ii) lightweight laminate sheets, i.e. with thickness composition of core $= 0.2\,mm - 1\,mm$ and skin $= 0.1\,mm - 0.4\,mm$. Moreover, there are a variety of polymers to be selected as the middle layer. Polypropylene [10], polyethylene [15], polyolefin (PP-PE) [7], and polyamide [16] are the most popular polymers used in three-layer laminates. The chief reasons for choosing these polymers are low density, good mechanical properties, good chemical stability, low cost, and high-temperature resistance [12]. These polymers usually have low wettability and bondability in contact with other surfaces due to their low-polarity behavior. Therefore, various adhesive films are used to attach the polymer core to metal adherends. Common adhesives used in the manufacturing of three-layer laminates are hot-melt polyethylene adhesive film [8], maleic polyethylene adhesive film [9], Ethylene-Vinyl Acetate (EVA) film [10], epoxy resin (koratac FL 201) [17] and PolyproPylene Grafted Maleic Anhydride (PP-G-MA) thin film [18]. Due to the indirect bonding of the metal to the polymer and the presence of an additional layer and subsequently the dependence of metal/polymer interface strength on adhesive strength, and considering the subsequent mechanical and metallurgical processes, appropriate selection of the adhesive is crucial. In some studies, adhesives have been used directly as an intermediate layer (without the polymer core) between two metals [13]. The results show that the presence of adhesive between the two steel layers, while improving the laminate elongation, and delaying the necking, increases the formability of the three-layer sheet compared to the two-layer sheet without the adhesive. Adhesive bonding (manual lamination) [19], hot [17] and cold roll bonding [20], and hot pressing [9] are well-known processes in the production of metal/polymer/metal laminates. Carrado et al. [1], by comparing the roll bonded and hot-press bonded specimens of the same thickness, showed that the initial crack strength of the rolled sheet was higher than that of the hot-pressed sheet. Kazemi et al. [9] applied three-point bending test on the aluminum/polyurethan/aluminum three-layer sheet produced by the hot-pressing method. They related the debonding observed in the interface of aluminum/polyethylene to the creation, growth, and connection of micro-voids formed on the polymer surface during the hot pressing. The thickness and physical and mechanical properties of the polymer core and the bond strength affect the mechanical properties, formability, paintability, and weldability of the three-layer laminates sheet. Harhash et al. [7] reported the decrease in density and subsequently weight-saving as a positive and decrease in tensile and yield strength as an adverse effect of increasing the volume fraction of the polymer in the three-layer composite sheets (constant skins thickness). The importance of the polymeric layer shear strength is revealed where the shear force generated between the skin layers during the various forming processes (bending, drawing, etc.) overcomes the shear strength

of the polymer and interfacial delamination occurs. It was observed that weak polymer core causes skin sheets to slide on the other layer (lubricant-like behavior), resulting in a premature splitting [21]. By investigating the deep drawing process of the three-layer sheets with different polymer cores, Liu et al. [15] showed that the drawability of three-layer sheets becomes poor as the thickness and strength of the polymeric core increase. Kim et al. [10] attributed the improvement in the formability of the three-layer sheets to the high elongation of the polymer core and the high bond strength of the metal/polymer interface. It is demonstrated that for two laminate sheets of the same thickness and steel skins, the sheet with polypropylene core shows lower springback than the laminate with the Poly Vinyl Chloride (PVC) core [22]. This is attributed to higher strength of the PVC sheet compared to the polypropylene sheet. Since three-layer sheets in the car body are placed in the paint bath (temperature of 200°C for 30 minutes) after the forming stage, the polymeric core must have a melting temperature of more than 200°C to maintain its structure [23]. If the melting temperature of the polymer is less than the painting temperature, the polymer melts, and the flow of the polymer disturbs the structure of the part, and the paint bath becomes contaminated. Saito et al. [24] and Oberle et al. [25] in two separate investigations demonstrated that, since during spot welding process, the polymer core is heated and pressurized by the welding electrode, to improve the weldability of the three-layer sheet and the formation of an ideal weld, the polymer core must flow away from the welded area. As such, the flow properties of the polymeric core should be optimal so that the delamination does not occur in the composite during the welding and painting processes. Studies have shown that the surface treatment of the skin metal sheet such as corona treatment [1] and preheating plus wire brushing [26] effectively improves the surface energy and wettability and produces more contact surfaces. This leads to the enhancement of shear strength and formability of the three-layer sheet.

It is evident from the literature that the manufacture of multilayer composites is challenging because of significant differences in the mechanical properties and adhesion characteristics of polymeric core and metallic face sheets. This unique combination of materials requires advanced joining techniques to ensure a strong bond between the joining layers. Thus far, few studies have been carried out to consider the impact of fabrication methods, core volume fraction and orientation of Steel/Polymer/Steel (S/P/S) laminate sheets on its overall mechanical properties. Subsequently, considering that many parameters are involved in the manufacture and the final properties of this type of composite material systems, an exact evaluation is necessary to identify and achieve the mechanical properties of the composite for each specific application.

The present study holds significant implications for the field of metal/polymer composites and endeavors to bridge the gap in knowledge. It also contributes to advancing the understanding of the direct roll bonding process and provides valuable insights for further optimizing the fabrication process, leading to the development of novel S/P/S composites with improved performance for various applications in automotive, aerospace, and structural engineering.

Thus, in this research, S/P/S laminates are manufactured by the roll-bonding process, without the use of adhesives (or reinforcements) and heated rollers (section 2). The authors attempt to achieve optimal mechanical properties. Three variables are considered:

- The polymer layer thickness (volume fraction of the core material)
- The rolling speed
- The rolling direction

Single Lap Shear (SLS) and T-peel tests were carried out to obtain the best rolling speed value for fabrication of four different laminate thicknesses by comparing the results of shear and bond strength, respectively. The effect(s) of the core volume fraction and rolling direction on the mechanical properties of the S/P/S sheet was studied by performing the uniaxial tensile test. The results were analyzed by examining the obtained data and the Scanning Electron Microscope (SEM) and are presented in section 3. Finally, the findings of the present work are concluded in section 4.

II. Methodology

a) Laminate Manufacturing

The Aluminum Killed (AK) low carbon steel St14 having $0.45\ mm$ thickness was selected as the face sheet of the S/P/S laminate due to its good mechanical properties and excellent formability and weldability. The chemical composition of the St14 steel sheet is illustrated in Table 1. Furthermore, a Thermoplastic Polyurethane (TPU) sheet with an initial thickness of $2\ mm$ was employed as the middle layer (core) of the three-layer sandwich sheet. Selection of the TPU sheet was due to its remarkable tensile and tear strengths, exceptional impact resistance, high chemical and corrosion resistance, excellent ductility over a vast temperature range, low weight and cost, and ultra-high adhesion with various surfaces [27]. Due to the importance of the working temperature of thermo-mechanical processes and changes in the polymer behavior at different temperatures, it is essential to know the rheology of the polymer. Thus, the Differential Scanning Calorimetry (DSC) analysis was performed on the TPU to determine the working temperature. The DSC curve of the TPU shows an endothermic peak at $226°C$ associated with the melting temperature (T_m), as shown

in Figure 1. The DSC curve of the TPU usually shows two glass transitions at $-40°C$ and $95°C$ related to the soft and hard segments (T_g^{SS} and T_g^{HS}), respectively [10], [22], [28]. Accordingly, the working temperature of this study was chosen between the highest glass transition (T_g^{HS}) and the melting temperature (T_m).

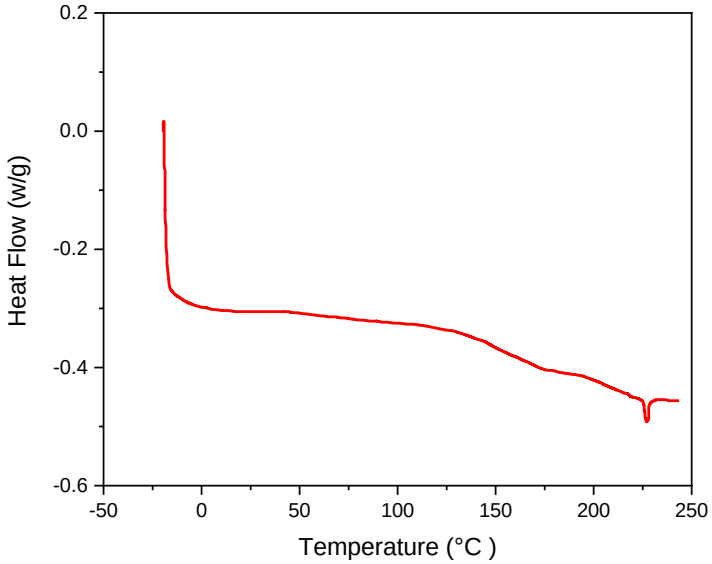

Figure 1: DSC curve of the TPU

Table 1: Chemical composition of the steel sheet

Fe	C *	Si	P	S	Cr	Ni	Mn	Mo	Al
Base	0.090	0.020	0.010	0.005	0.012	0.030	0.300	0.030	0.040

** numbers are in %*

The three-layer S/P/S laminates were manufactured by the roll bonding process, without any adhesive or reinforcement. The following steps were conducted in hierarchal order:

I. To increase the adhesion strength, the inner surfaces of both skin steel sheets were roughened in the rolling direction of sheet using stainless steel wire brush. Surface roughness was perfectly uniform and was measured by the Pocket-Surf®III roughness measuring mobile instrument after each brushing step. Post brushing, the average surface roughness of the St14 sheet was $R_a = 3.63\,\mu m$. The optical graph of the brushed steel surface is shown in Figure 2.
II. The contact surfaces (brushed side) of the two skin sheets and both sides of the TPU sheet were washed with acetone. The surfaces were air-dried to remove the surface contaminants and improve the quality of the bond.
III. The TPU sheet was sandwiched between the two skin face sheets. The four corners of the laminated sheet were punched to prevent slipping of the layers during the process.
IV. The unbonded laminate was placed at $200°C$ fixed temperature oven for 5 minutes. The goal was to semi-melt the polymer to ease penetration of the rough surfaces into TPU surfaces leading to enhancement of the bond strength.
V. The sample was rolled immediately after removal from the oven to achieve the desired thickness. Considering the thickness of the unbonded laminate ($2.9\,mm$), the three-layer laminates were fabricated at three rolling speeds and four rolling thickness reductions. The naming of test laminates was based on corresponding rolling speeds and thickness reductions, respectively (see Table 2). The cross-sectional view of four laminates with various thicknesses is presented in Figure 3.

b) Evaluation of the Mechanical Properties of the Base Sheets

To investigate the mechanical properties of metal and polymer sheets and compare them with different laminates, the uniaxial tensile test specimens were prepared according to ASTM E8/E8M and ASTM D638 (type IV) standards for steel and polymer sheets, respectively. Tensile tests of the steel sheet specimens along the rolling (RD), diagonal (DD), and transverse

(TD) directions, were conducted by the Hounsfield H10NKS machine with the test speed of $1\ mm/min$. The mechanical behavior of the TPU sheet was also obtained by the same machine with the test speed of $50\ mm/min$. Repeatability of the results was assured by performing at least three tensile tests for each condition. Due to the importance of the polymer tear strength under tension and shear conditions, the tear strength test was conducted on the TPU sheet according to ASTM D624-00 (type C) standard and with the crosshead speed of $50\ mm/min$. It is worth noting that all tests were performed at room temperature.

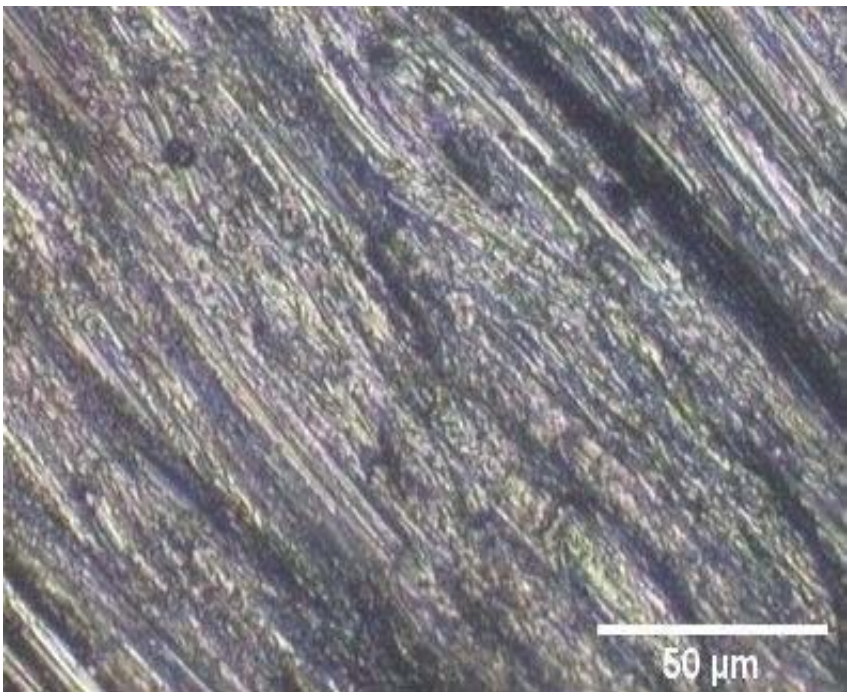

Figure 2: The optical micrograph of the roughened surface

Table 2: The laminates parameters and naming

Thickness Reduction (%)	Total Thickness (mm)	Core Volume Fraction (%)	Rolling Speed (rpm)		
			25	35	40
			Laminate Naming		
30	2.03	55.6	L-25-30	L-35-30	L-40-30
40	1.74	48.2	L-25-40	L-35-40	L-40-40
50	1.45	37.6	L-25-50	L-35-50	L-40-50
60	1.16	22.4	L-25-60	L-35-60	L-40-60

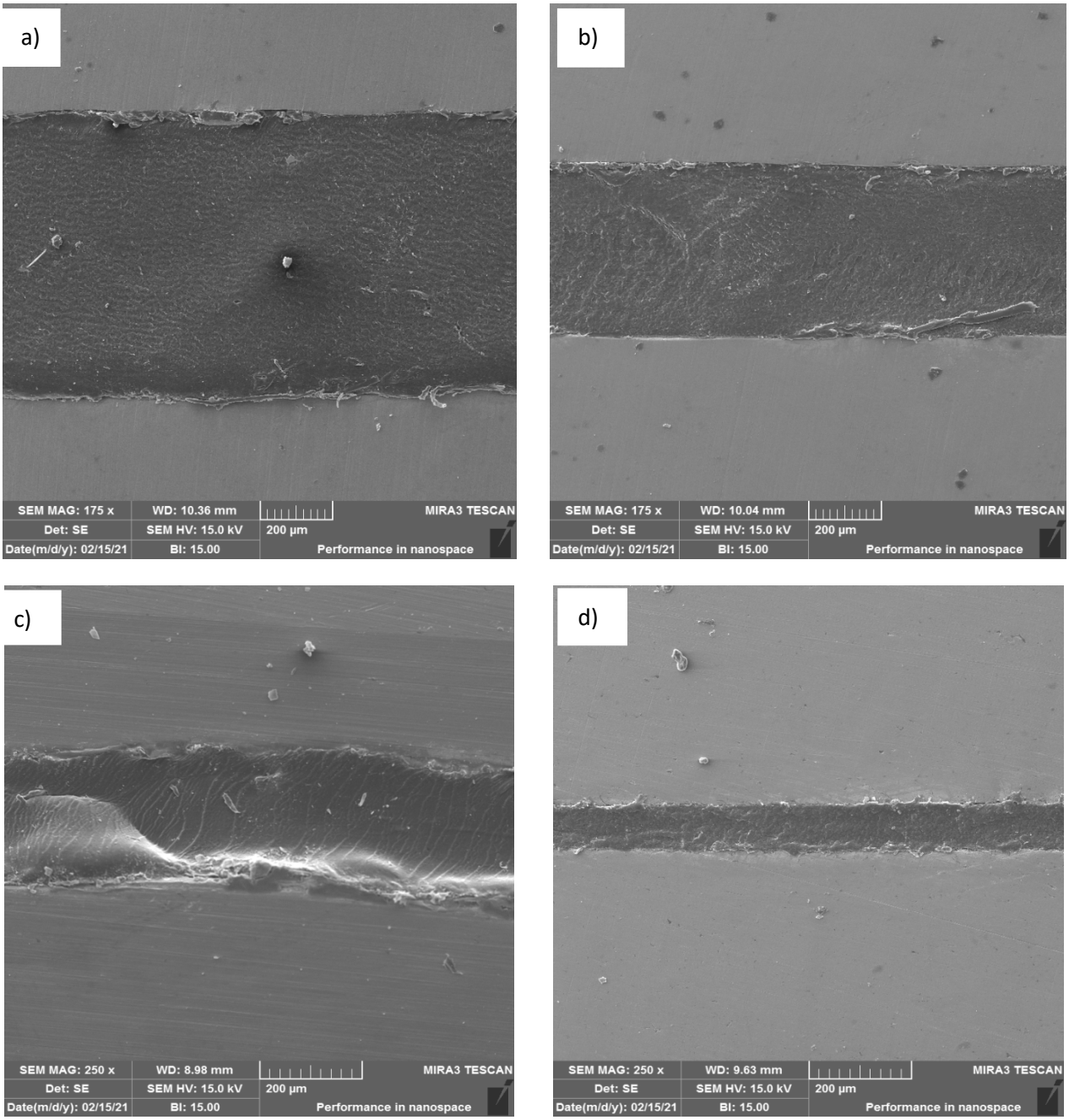

Figure 3: Cross sectional view of various laminates; (a) 30%, (b) 40%, (c) 50%, and (d) 60% thickness reduction

c) Rolling Speed Characterization

The optimal rolling speed is a key factor that has a significant impact on both the interfacial strength and fabrication of the three-layer laminates. Moreover, It can influence the mechanical and physical properties [29]. To determine the optimum rolling speed, bonding evaluation tests were carried out [30]. To evaluate the bond strength at skin-core interface of the different laminates under normal loading conditions, the T-peel and SLS tests were used. The T-peel test was performed according to the ASTM D1876-08 with the test speed of $20\,mm/min$. On the other hand, the SLS test was conducted according to ASTM D-3165-07 with the crosshead speed of $1\,mm/min$ to reflect the shear mechanical properties of the polymer layer. Figure 4 shows the geometric parameters of the T-peel and Lap-shear specimens. The size of specimens was modified in the small range. Due to the sensitivity of the results of these two tests and aiming to assure the accuracy of the results, the tests were repeated five times for each sample and the average values are reported.

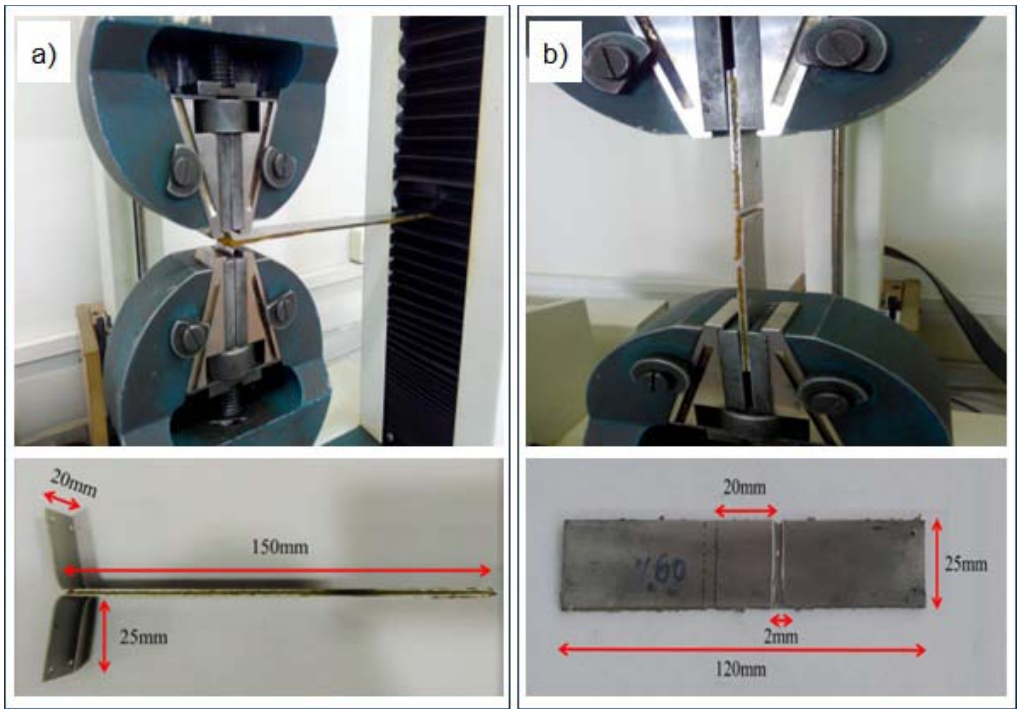

Figure 4: Experimental test set up and size of specimens for a) T-peel test and b) Single Lap Shear (SLS) test

d) Characterization of the Mechanical Properties of the Laminates

To study the impact of the core volume fraction and rolling direction on mechanical properties of three-layer laminates and its comparison with the monolithic steel sheet, the uniaxial tensile test was designed at three directions (RD, DD, and TD). To that end, the ASTM E8/E8M standard test method and constant crosshead speeds of $1\,mm/min$ were chosen. Repeatability of the results was assured by performing at least three tensile tests for each direction, i.e. a total of 9 tensile tests.

e) Analysis of the Results

Due to thickness reduction of the polymeric core during the thermomechanical process and its impact on polymer microstructure, the density of different laminates may be different. Therefore, this property was experimentally investigated using a measuring cylinder and laboratory digital scale.

The experimental results were compared with those predicted using the rule of mixture for laminates [31]:

$$P_{SMS} = P_{Skin} \times V_{Skin} + P_{Core} \times V_{Core} \quad (1)$$

where P_{SMS} is the specific property of the laminate sheet, P_{Skin} and P_{Core} are that property for the skin sheet and polymeric core, respectively. V_{Skin} and V_{Core} are volume fractions of the skin sheet and polymeric core, respectively.

The bonding interface of the St14/TPU/St14 laminate sheet was investigated by using the Scanning Electron Microscope (SEM). Furthermore, the SEM was utilized to examine the fracture surface of the specimens after performing the T-peel and SLS tests.

III. Results and Discussions

a) Mechanical Properties of the Core Sheet

Since the mechanical properties of the core and the skin face sheets control the mechanical properties of three-layer laminates, a precise study of their mechanical behavior is required. Figure 5 shows the typical true strain-stress curve of the $2\,mm$ thick TPU sheet.

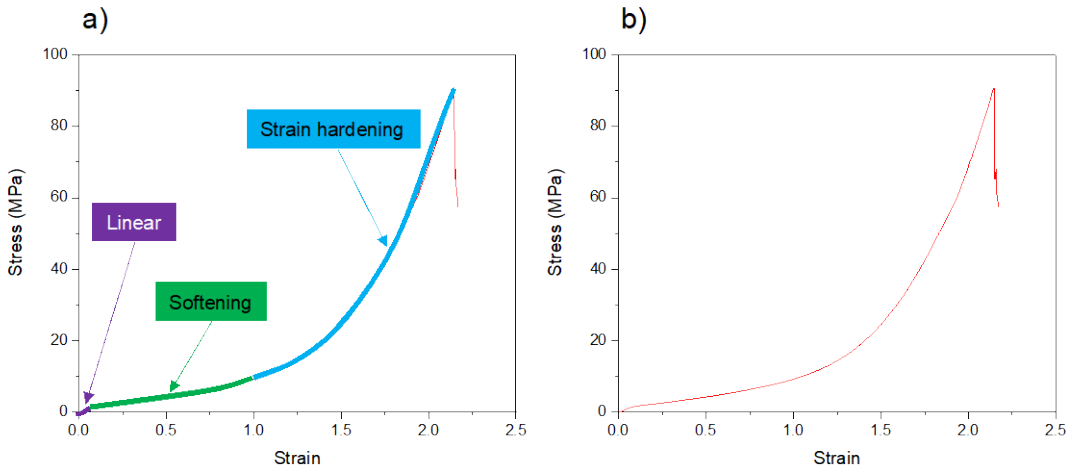

Figure 5: Stress-strain curve of the TPU sheet, a) characteristic areas of the graph, b) true stress-strain curve

The stress-strain behavior of the TPU is divided into three stages [32] as shown in Figure 5a. For the small strains, the curve is almost linear (purple region), and the specimen exhibits relatively stiff behavior. Material softening is the second phenomenon at the medium strain level (green region), and finally, strain hardening evolves progressively due to the strain-induced crystallization phenomenon at the largest strain (blue region). The combination of these three stages leads to the high strength of the polymer while maintaining considerably large elongation up to the point of failure.

The possibility of cutting, necking, and rupturing of the polyurethane sheet under tension or shear loading, increases the importance of the tear strength. The load-extension curve obtained from the tear test which is performed according to ASTM D-624-00 (Type C) is shown in Figure 6.

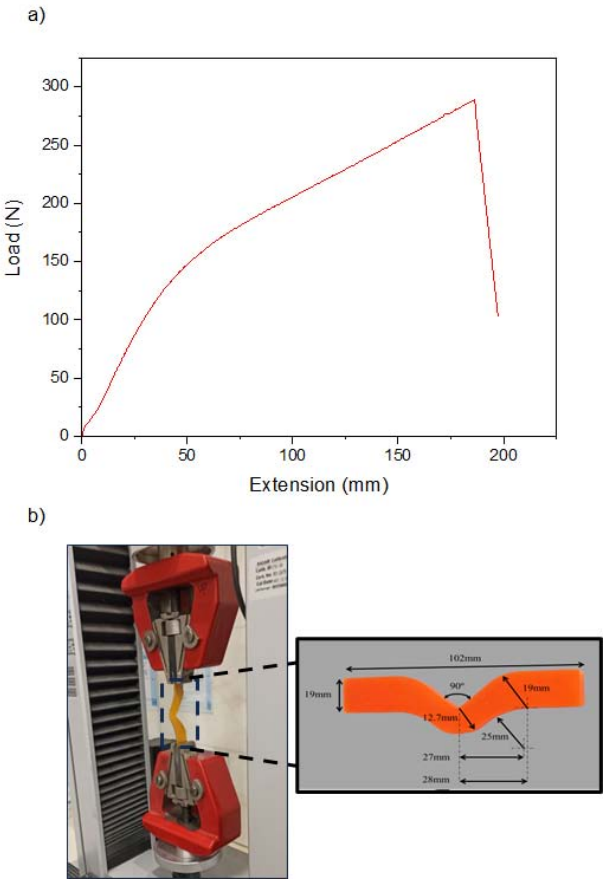

Figure 6: Illustration of tear test set up, a) Tear strength curve of the polymeric sheet, b) the experimental setup, and c) Dimensions of the sample based on ASTM D-624 (type C)

The change in the slope of the curve in the $50\,mm$ extension is due to the change of loading conditions in the torn region of the test specimen. Tear strength of the TPU sheet is defined as the ratio of maximum load ($286\,N$) at fracture point ($\approx 186\,mm$ extension) to the thickness of the specimen ($2\,mm$). Therefore, the tear strength of $\approx 143\,N/mm$ indicates high resistance of the TPU sheet to local deformation, and he extended tearing time (≈ 223 seconds) proves their superior level of stretchability, and excellent elongation.

b) The Optimum Rolling Speed of S/P/S Laminate

T-peel and SLS tests were performed on different laminates to determine the optimal rolling speed. T-peel test and SLS test data reflect the normal and shear mechanical properties of the laminates, respectively. Hence, by evaluating and comparing the results of these tests, it is possible to determine the optimal rolling speed for fabricating the maximum-bond-strength laminates for further experiments. The typical load-extension curves resulted from the T-peel and the SLS tests are illustrated in Figure 7.

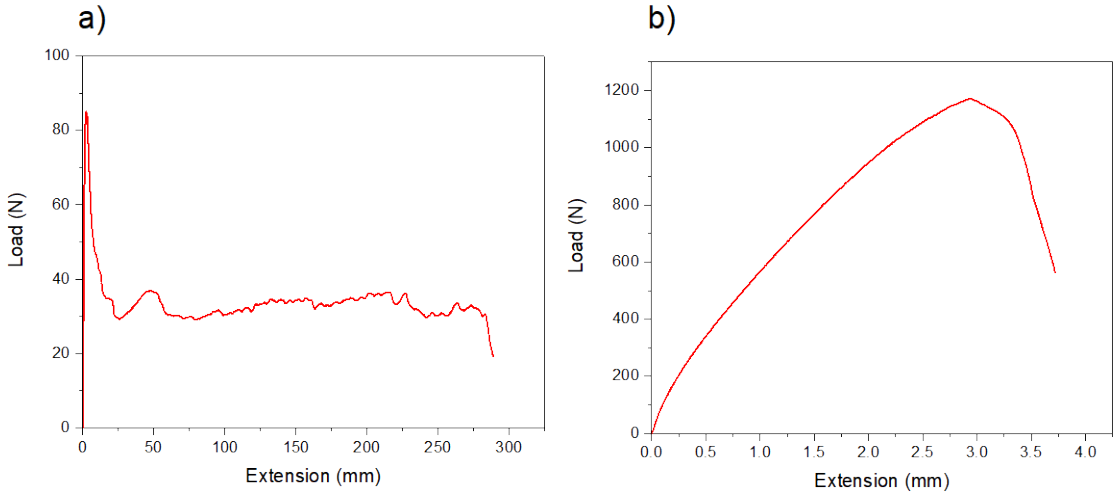

Figure 7: Load versus extension of, a) a T-peel test and b) SLS test

The Average Peel Strength (APS) can be calculated by [26]:

$$APS = {averageload\ (N)}/{bondwidth\ (mm)} \qquad (2)$$

where the average load is the average stable peel force after the first peak load.

Figure 8 shows the average peel strength at three various rolling speeds for four different laminates. Based on the figure, the bond strength decreases with increasing the rolling speed. The high bond strength at low rolling speed can be related to the longer time that the sample passes through the rollers. In general, in the rolling process of metallic sheets and composites which consists of two or more metallic sheets, the rolling speed before and after rolling (at the entrance and exit points) is not equal due to the occurrence of thickness reduction in the samples. In S/P/S laminates due to the fact that thickness reduction is only on the semi-melted polymericlayer and the steel sheets pass through the rollers without any reduction in thickness, it can be assumed that in the rolling process of S/P/S laminates, the initial and final velocity of the rollers is equal. Therefore, by converting the angular rolling speed to linear speed, it is possible to obtain the time that the samples pass through the rollers.

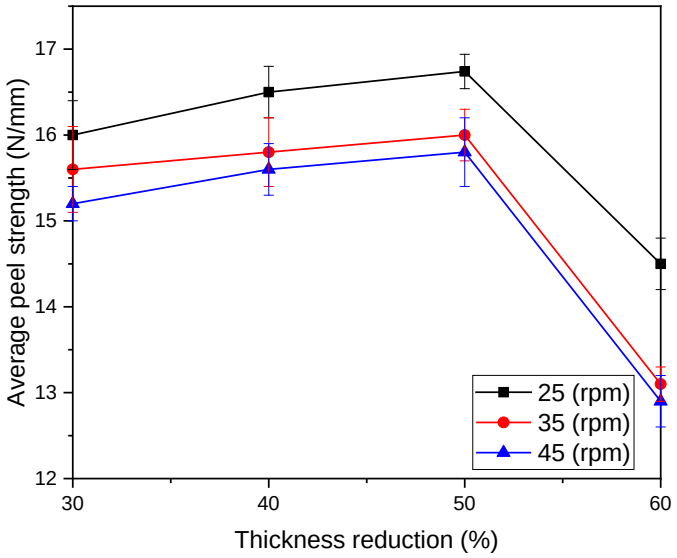

Figure 8: Comparison of the average peel strength at three various rolling speeds for four different laminate

The passage time is calculated by the following equation:

$$T = {}^{L \times 60}/_{V \times P} \quad (3)$$

Where T represents the passage time (s), L is the sample length (mm), V is the angular rolling speed (rpm), and P is the roller perimeter. Figure 9 illustrates the schematic view of the roll bonding process of S/P/S laminates including these parameters.

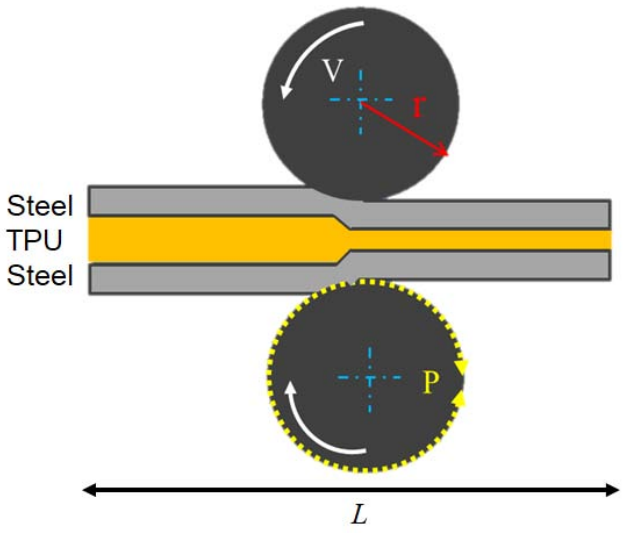

Figure 9: Schematic illustration of the roll bonding process

Therefore, the passage time of a $15\ cm$ long T-peel sample between two rollers with a diameter of $15\ cm$ at rolling speeds of 25, 35 and $45\ rpm$ is 0.76, 0.54, and 0.42 seconds, respectively. This longer passage time guarantees uniform flow of the semi-melted polymer in the rolling direction between the two face sheets. Additionally, the low rolling speed prevents displacement and unwanted sliding of the two face sheets relative to each other and ensures the structural integrity of the laminates. Any sliding and movement of the face sheets relative to each other, which is probable at higher rolling speeds, can prevent the smooth flowing of the semi-melted polymer between them leading to formation of the cavities resulting in weakening of the bond strength. Therefore, the coincidence of brushed surfaces in rolling direction provides ducts for polymer flow in the same direction. This results in more engagement between the polymer and the roughened surfaces of the steel sheets. Consequently, this leads to improvement of the bond strength and minimizes the risk of delamination or separation. Andani et al. [33] have reported that the probability of formation of cavities at metal-polymer interface is higher as the semi-melted polymer flowed outside the laminate structure resulting in decreasing the bond strength. These cavities were formed in samples that were wire brushed first in the rolling direction and then perpendicular to the rolling direction. Therefore, it can be concluded that the smooth flow of the polymer in one direction can prevent the formation of these cavities and promote the cohesion of the bond.

At the exit of the rolling machine, the final temperature of the laminates that rolled at high rolling speed is higher than that of those rolled at low rolling speed. This is due to the short contact time of the preheated sample with the cold rollers. This

phenomenon elevates the potential of the generation of interlayer cavities by giving the warm polymer adequate time to undergo a gradual cooling process without the presence of external pressure. Andani et al. [33] demonstrated that at high rolling speed, the high temperature of the sample causes the polymer to become excessively soft, and the removal of the polymer from the sandwich structure is easier. Thus, there is not enough time for the polymer to penetrate the roughened surfaces, and consequently the bond strength decreases.

Furthermore, as Abbasi and Toroghinejad [34] observed, higher rolling speeds lead to shorter bond times to effectively apply pressure on the rolled sheets resulting in a sharp decrease in the adhesion strength. Thus, as the rolling speed decreases, the contact time increases. Increasing the effective pressure of the rollers which is obtained by lowering the rolling speed, facilitates the squeezing, extruding, and penetrating of the semi-melt polyurethane into the brushed surface of skin sheets resulting in effective integration and generation of more mechanical interlocks.

Observation of the T-peel specimens after performing the test revealed both cohesive failure (fracture within the polymeric core) and adhesive failure (fracture along the interface between the polymeric core and skin sheets) modes. Samples with cohesive failure were associated to the result of optimum thickness reduction and low rolling speed, whereas the samples having adhesive failure were the result of suboptimal thickness reduction and high rolling speed (Figure 10).

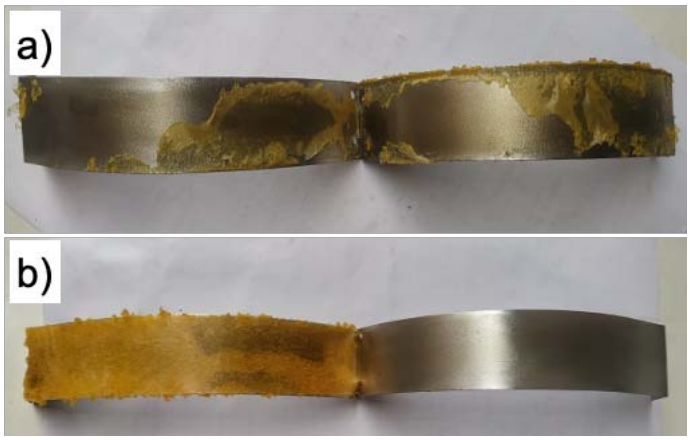

Figure 10: Failure of specimens after T-peel test, a) cohesive failure and (b) adhesive failure

Figure 11 shows the shear strength of S/P/S laminate for various thickness reductions. In this graph, the shear stress is calculated as:

$$\tau = {}^{F_{max}}/_{A} \quad (4)$$

Where F_{max} and A are the maximum load and the overlap area ($400\ mm^2$), respectively. As shown in Figure 11, increase in rolling speed leads to reduction in shear strength. Moreover, for all rolling speeds, as the thickness of S/P/S laminates decreases (up to 50% thickness reduction), the single lap shear strength increases. This is attributed to the fact that thinner laminates have smaller load eccentricity. As such, joint bending moment caused by load eccentricity decreases leading to less peel stress at steel-polymer interface. It can be inferred that in S/P/S laminates, the volume fraction of micro pores and cavities and interfacial toughening, contribute to the resistance of the metal-polymer interface against crack initiation and propagation. In laminates with a high polymer volume fraction, the larger volume of micro pores and cavities within the polymer structure surpasses the benefits of interfacial toughening, subsequently reducing the resistance of the metal-polymer interface to crack propagation. Conversely, in laminates with a low volume fraction of core material, although the volume of micro pores and cavities in the polymer structure is smaller, interfacial toughening is minimal, resulting in easier crack propagation. Therefore, achieving the highest level of crack resistance at metal-polymer interface requires optimizing both the volume fraction of micro-pores and the degree of interfacial toughening. Additionally, the optimum thickness of the core acts as a stress-absorbing element, effectively preventing crack initiation and arresting crack propagation at the interface, thereby improving the overall shear strength of the laminate. It is worth noting that laminates with 50% thickness reduction showed higher normal strength in T-peel test (see Figure 8). Hence, it could be inferred that, by striking a balance between interfacial toughening and the volume fraction of micro-cavities, laminates with a 50% thickness reduction exhibit the highest shear strength.

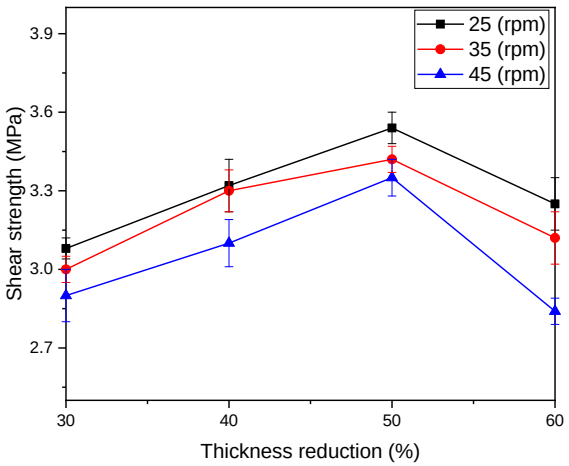

Figure 11: Comparison of the shear strength at three various rolling speeds for four different laminates

Figure 12 shows the fracture surfaces of the two SLS test specimens at the same thickness reduction (40%) at two rolling speeds of 25 rpm and 45 rpm. The magnitude of effective pressure applied to the specimen controls the volume fraction of the micro-cavities at the metal-polymer interface. It is suspected that there is an inverse correlation between the volume fraction of the micro-cavities at the metal-polymer interface and the effective contact surface and subsequently the bond strength of the laminates. In other words, the higher metal-polymer interfacial volume fraction leads to low bond strength due to lower effective contact surface. Furthermore, lower rolling speeds are accompanied by higher effective pressure on the specimens, better penetration of the polymer to the rough surfaces of the skins, and thus reduction in volume fraction of the metal-polymer interfacial micro-cavities.

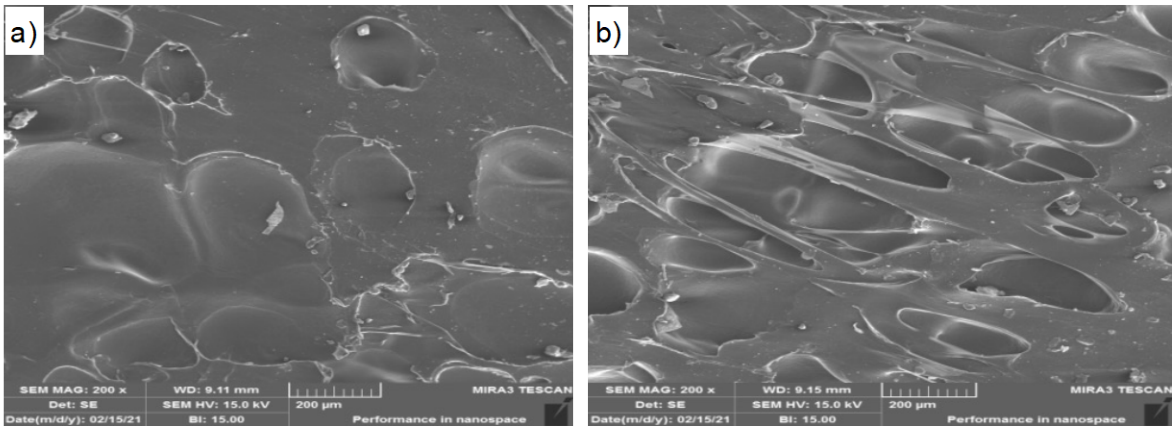

Figure 12: Fracture surfaces of the single lap shear specimens fabricated at rolling speed of: a) 25 rpm and b) 45 rpm

c) Mechanical Properties of the Laminate and Monolithic Steel Sheet

In this section, the effects of sample direction and volume fraction on the mechanical properties of laminates are discussed. The results provided hereafter are for steel sheet and four different laminates fabricated at optimum rolling speed of 25 rpm in three directions with respect to the rolling direction.

i. *Effect of the Sample Direction*

Figure 13 compares the typical stress-strain curve of both monolithic steel sheet (0.45 mm) and a specific Steel/Polymer/Steel sheet (0.45/0.26/0.45 mm) under uniaxial tensile loading. Both materials initially display linear elastic behavior. Generally, the stress-strain curve of the laminate displays a more gradual transition from the elastic region to plastic deformation compared to that of a monolithic. As the steel sheet approaches ultimate failure, it exhibits a more abrupt necking behavior, resulting in a relatively sharp drop in stress. This brittle failure is characteristic of metallic materials, where the strong atomic bonds lead to sudden fracture under high strain. In contrast, the presence of the polymer layer in the S/P/S laminate

introduces a ductile behavior that enhances toughness and prevents rapid failure. The polymer layer provides additional energy absorption and deformation capacity, resulting in a more gradual and controlled stress reduction prior to failure.

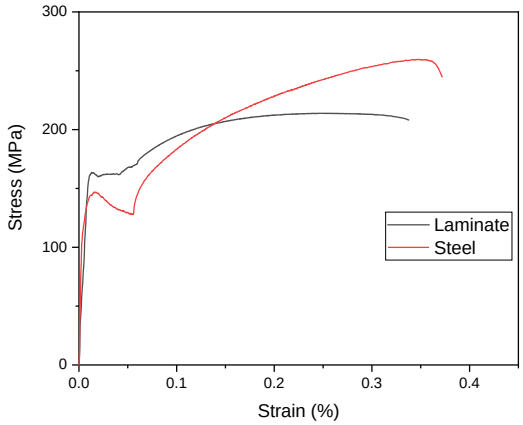

Figure 13: Stress-Strain curve of monolithic and laminated steel sheets

Figure 14 and Figure 15 show the yield and ultimate strength of laminates for various sample orientations with respect to RD and various thickness reductions, respectively.

As shown in the figures, there are considerable differences in the yield and ultimate tensile strengths for all four laminates compared to the monolithic steel sheet. Based on Figure 14, the yield strength of the monolithic steel sheet at all three directions (RD, DD, and TD) is higher than the three laminates L-25-30, L-25-40, and L-25-50. However, the yield strength of L-25-60 laminate is higher than that of the steel sheet. Similarity of the trends of L-25-50 and L-25-60 to the steel sheet curve suggests that the yield behavior of the thinner laminates is closer to that of the skin sheet due to reduced influence of polymer layer. While the polymer layer still contributes to factors such as interfacial adhesion and other mechanical properties of laminate, its influence on the overall yield behavior diminishes as laminate thickness decreases. Increasing the volume fraction of the polymer leads to the same yield behavior in three directions.

Comparison of the results of Figure 15 shows that the tensile strength of the monolithic steel sheet in the DD is higher than that of all other laminates. However, for both RD and TD, the tensile strength of the steel sheet is lower than the L-25-60 and more than L-25-30, L-25-40, and L-25-50 laminates. The same trend of the steel sheet curve and all laminates exhibit the high dependence of the tensile strength of the laminates on the tensile strength of the skin sheets in all three directions. Consequently, this finding suggests that the mechanical properties of the steel face sheets exert a relatively greater impact on the UTS of the laminate compared to the polymeric core.

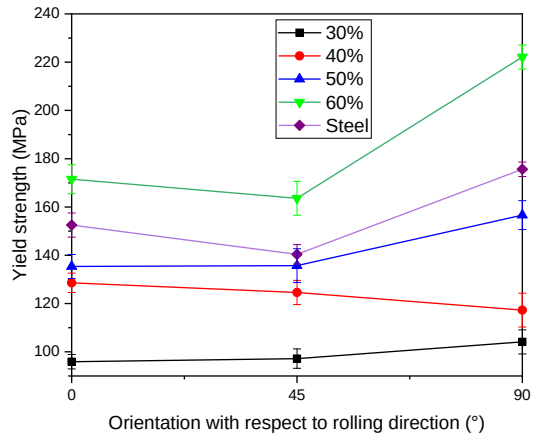

Figure 14: Effect of the angle of the sample axis with respect to RD on the yield strength (for various thickness reductions and bars on data points shows standard deviation of the test samples)

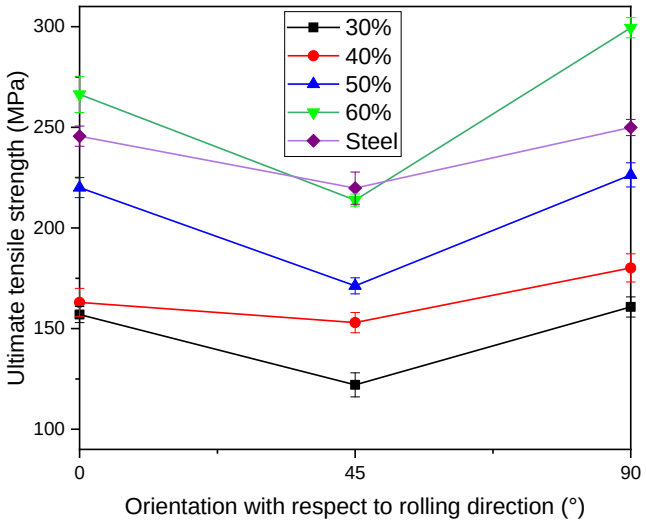

Figure 15: Effect of the angle of the sample axis with respect to RD on the ultimate tensile strength (for various thickness reductions and bars on data points shows standard deviation of the test samples)

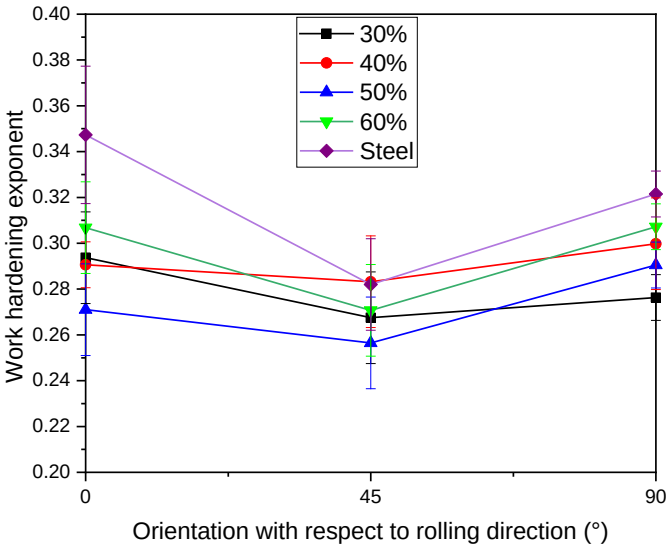

Figure 16: Effect of the angle of the sample axis with respect to RD on the work hardening exponent (for various thickness reductions and bars on data points shows standard deviation of the test samples)

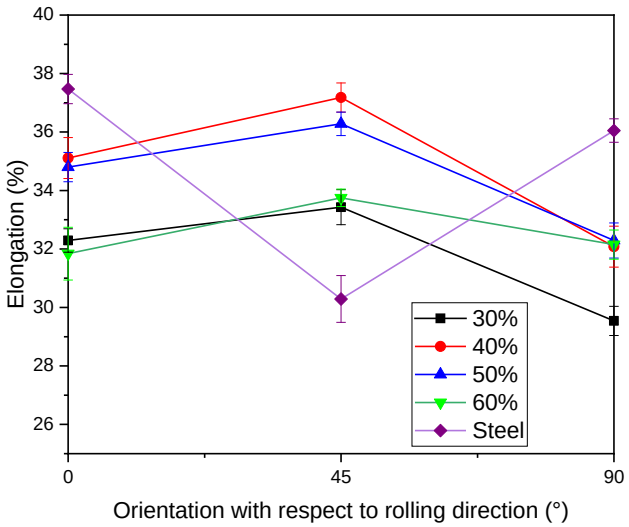

Figure 17: Effect of the angle of the sample axis with respect to RD on the ultimate elongation (for various thickness reductions and bars on data points shows standard deviation of the test samples)

The work hardening exponent measures the extent to which the material (monolithic and laminated steel sheet) undergo work hardening in response to uniaxial tensile load. Based on Considère criterion, the true strain (at maximum force) equates to the strain hardening exponent ($\varepsilon_u = n$) at the onset of localized necking. The work hardening exponent parameter of both monolithic steel and S/P/S laminate is given in Figure 16. Based on the figure, the n value of monolithic steel face sheet in RD and TD directions is higher than that of all S/P/S laminates. Besides, in DD direction, n of monolithic steel face sheet is approximately equal to that of L-25-40 and higher than that of other laminates. It is worth noting that DiCello [35] attributed the low work hardening exponent of the laminate compared to that of skin face sheet to the thermal aging of the metal skin during the lamination process. On the other hand, Harhash et al. [7] and Forcellese and Simoncini [36] attributed such a result to the soft polymer core which negatively affects the strengthening behavior of the laminate sheets. Furthermore, according to the study by Kim et al. [10], the strain hardening exponent of the polypropylene was reported to be lower compared to that of the AA5182 skin. This resulted in the reduction of the overall strain-hardening exponent of the sandwich sheets compared to monolithic aluminum sheet.

By changing the direction of the tensile samples of all laminates from $0°$ to $45°$, the work hardening exponent decreases. Then, the n value increases from $45°$ to $90°$. The same trend of n value at three directions for the monolithic steel sheet indicates that the work hardening exponent of laminates is dependent on the skinsheet.

As shown in Figure 17, by increasing the angular orientation of the tensile samples from $0°$ to $90°$, the elongation of all laminates first increases and then decreases while the skin sheet shows the opposite trend. Because the thicknesses of two skins of a laminate are equal and with same pressure on both sides of the polymer core, the metal-polymer interface strength of both sides is equal. It is suspected that, the occurrence of simultaneous necking of two steel skins in the same place increases the possibility of the premature fracture relative to the monolithic steel sheet. This simultaneous necking indicates a strong interaction between the skin layers, where they undergo a synchronized deformation mechanism. It can be influenced by various factors, such as the properties of the skin and polymer materials, their thicknesses, and the bonding strength between layers. At the DD, there is an improvement of this property for laminates. This can be related to high load bearing capacity (the ability of this specimen in distributing stress throughout the specimen length) of the metal-polymer interface samples at this direction. Forcellese and Simoncini [36] reported highest ultimate elongation value and post-necking deformation at $45°$ and similar elongation values for the $0°$ and $90°$ directions as well as lower post-necking deformation. They related this behavior to the lowest attitude to thinning owing to the highest normal anisotropy of the S/P/S sandwich composite occurring in the $45°$ angular orientation. Consequently, they observed the higher formability of samples at $45°$ orientation in the plane strain and drawing regions of Forming Limit Diagrams (FLD). Due to the significant difference between the elongation of the three-layer laminates and polymeric sheet, it can be concluded that

the two skin sheets strongly affect the three-layer sheet ductility behavior.

Figure 18 shows the Young's modulus (E, slope of linear portion of stress-strain curve) of S/P/S laminates and monolithic steel for various rolling directions. Based on the graph, E of S/P/S are lower than that of monolithic steel sheet for all rolling directions. Furthermore, the value of E is insensitive to the rolling direction for all laminates and monolithic steel. This indicates that, in the present study, S/P/S laminates demonstrate an isotropic and macroscopically homogenous behavior.

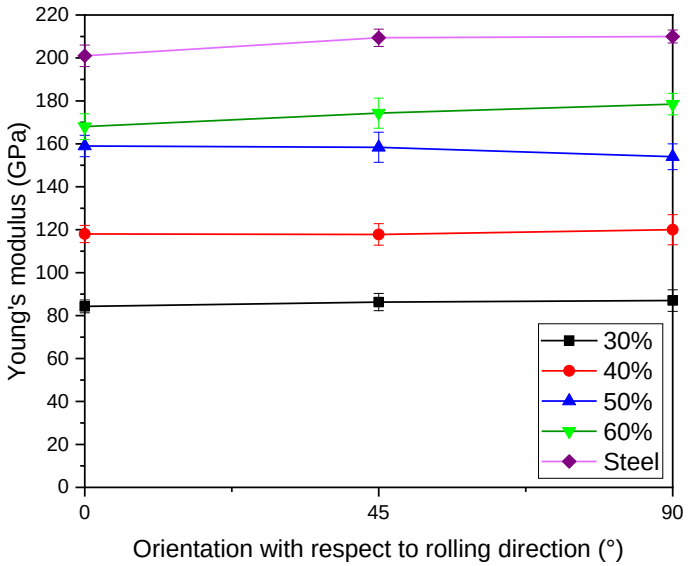

Figure 18: Effect of the angle of the sample axis with respect to RD on the Young's modulus (for various thickness reductions and bars on data points shows standard deviation of the test samples)

ii. *Effect of the Polymer Volume Fraction*

Figure 14 and Figure 15 show the increase in yield and tensile strength by decreasing the volume fraction of the polymer. Such result is in excellent agreement with those observed by Carrado et al. [1] and Harhash et al. [7].

Figure 19 shows the interface micrograph of all four laminates after lamination. According to the figure and the results of T-peel test (Figure 8), the mechanical interlocks have occurred between the rough surface of the skin sheet and the soft surface of the core sheet. This led to high bond strength at metal-polymer interface hindering the formation of delamination under tensile loading. On the other hand, the high tear strength of the polymeric sheet guarantees non-tearing along the width of the core sheet in the laminate structure. Therefore, all four laminates perform as an integrated sandwich structure. According to Figure 20, the ultimate tensile strength obtained from the tensile test (in the rolling direction) for two laminates L-25-50 and L-25-60 is higher than the calculated values obtained by the Rule Of Mixture (ROM). However, for L-25-30 and L-25-40, the experimental tensile strengths are lower than those obtained by ROM. It is observed that as the volume fraction of the polymer increases, the difference between the experimental and predicted tensile strength decreases commensurately.

It should be noted that there is not a clear correlation between the polymer volume fraction and the work hardening exponent (Figure 16).The similarity of results of all four laminates at all three directions to those of the monolithic steel sheet indicates that S/P/S laminates have high strain distribution behavior and consequently possess high formability.

Additionally, the highest elongation at all rolling directions belongs to L-25-40 and L-25-50 (Figure 17). The high bond strength of these laminates can be the reason of high elongation and consequently their delayed fracture. A similar conclusion was reached in [19].

Figure 18 indicates that increasing the thickness of the polymeric core leads to a decrease in the Young's modulus of the S/P/S laminates. As the thickness of the polymeric core increases, the proportion of the steel layers decreases. The polymer layer, which typically has a lower Young's modulus than steel, becomes a larger component of the structure. As a result, the overall Young's modulus of the structure decreases. Young's modulus of S/M/S sandwich sheets are calculated following the rule of mixture based on the Young's modulus of St14 steel and TPU sheets which are

$209.4\ GPa$ and $12.35\ MPa$, respectively. Figure 21 exhibits the difference between experimental and ROM values of young's modulus of S/P/S samples in rolling direction. Since ROM does not account for the interfacial bonding strength, this difference can be attributed to interfacial properties of the laminates along with strain rate dependency of the TPU core.

Comparison of the experimental and predicted ROM results indicates that the higher the volume fraction of the polymer, the larger becomes the difference between the obtained and predicted elongations (Figure 22). Due to the lack of pressure on the laminated sheet during cooling, micro-cavities may form in the polymer structure. Thicker laminates have more microcavities due to their high polymer volume fraction. Increasing the difference between the experimental density and its predicted value by increasing the polymer volume fraction supports this hypothesis (Figure 23). The density of the monolithic steel and polymer sheets is $7.8\ {}^{gr}/_{cm^3}$ and $1.25\ {}^{gr}/_{cm^3}$, respectively.

Figure 24 shows the effect of core volume fraction on the specific stiffness (Young's modulus/ Density) of the S/P/S laminates and compares experimental and estimated (ROM) values. The lower specific stiffness of L25-30 may be due to the thicker core, which might not be as effective in distributing the load, especially when the core material has significantly lower stiffness (0.0096 GPa/g.cm^{-3}) than the skin sheets (26.84 GPa/g.cm^{-3}). L-25-40 and L-25-60 have specific stiffness values close to that of the steel skin sheet, suggesting effective load distribution and potentially good interfacial bonding. The highest specific stiffness of L-25-50 (28.95) could be due to an optimal combination of core thickness and material properties, maximizing the load distribution and minimizing stress concentrations. It can be concluded that L-25-50 is the sample with promising thickness combination, which maintains a reasonable weight saving in addition to higher specific stiffness. Harhash et al. [7] demonstrated that E/D of 316L/PP PE/316L decrease as core volume fraction increase due to dominant effect of the polymeric core.

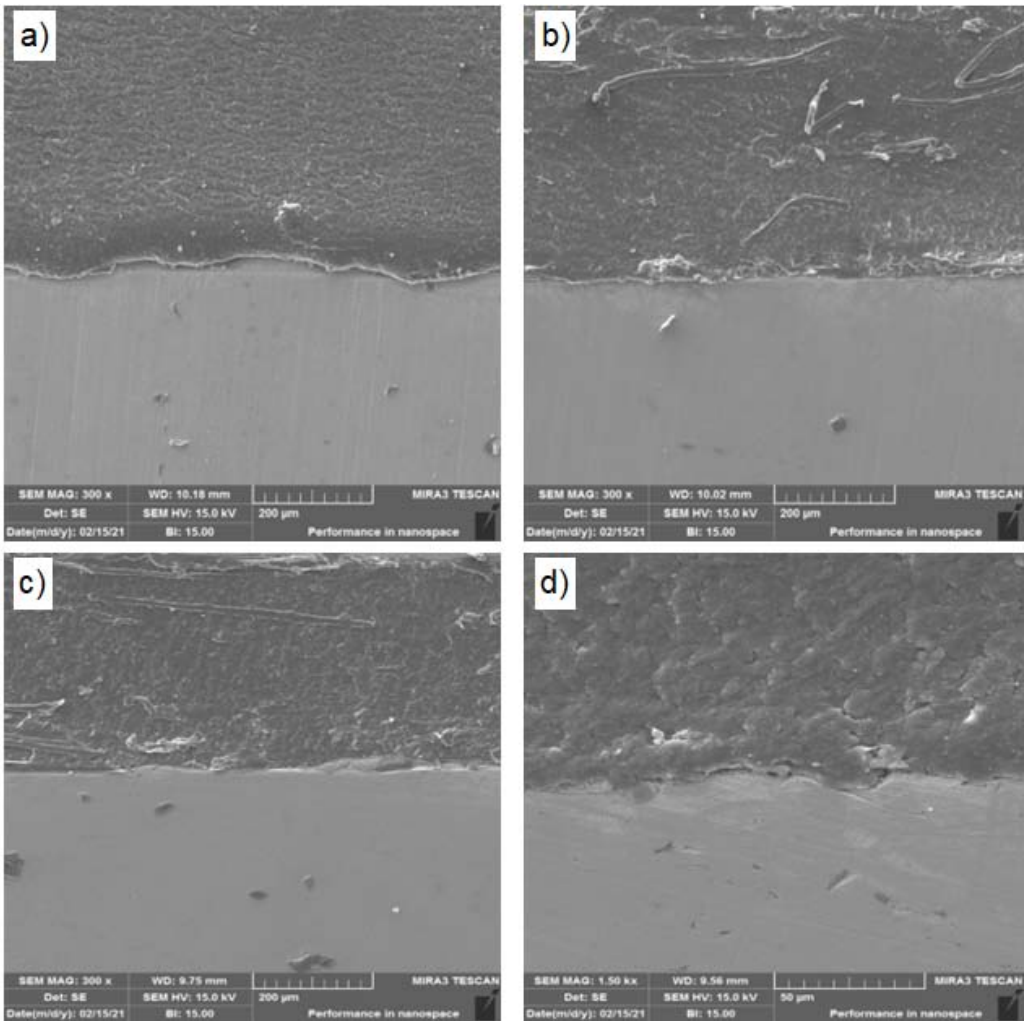

Figure 19: Metal/polymer interface of different laminates: (a) L-25-30, (b) L-25-40, (c) L-25-50, and (d) L-25-60 (Note: due to different thicknesses of specimens' different zooms and scales are used for each sample)

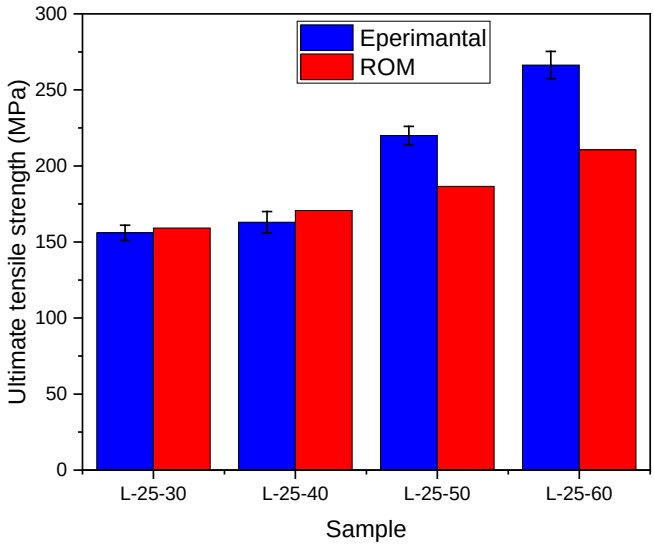

Figure 20: Comparison of the experimental and ROM results of UTS (at RD)

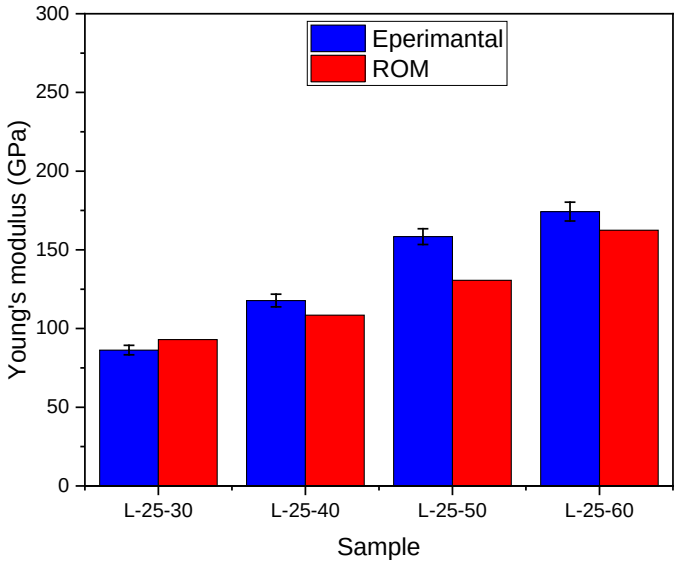

Figure 21: Comparison of the experimental and ROM results of young's modulus (at RD)

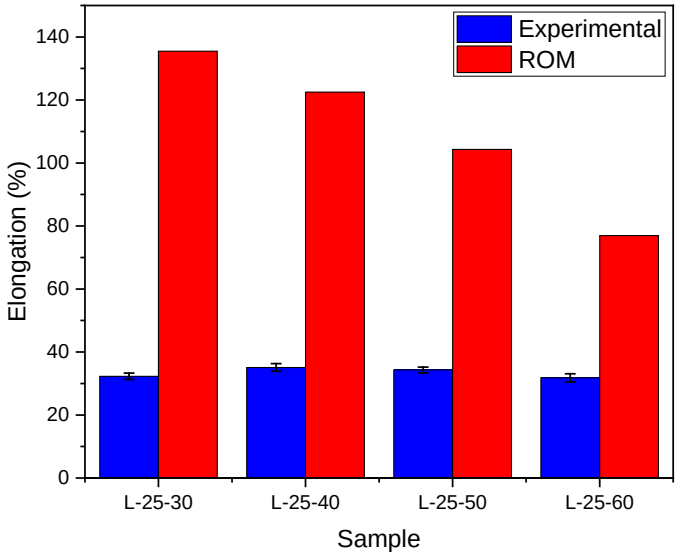

Figure 22: Comparison of the experimental and ROM results of elongation (at RD)

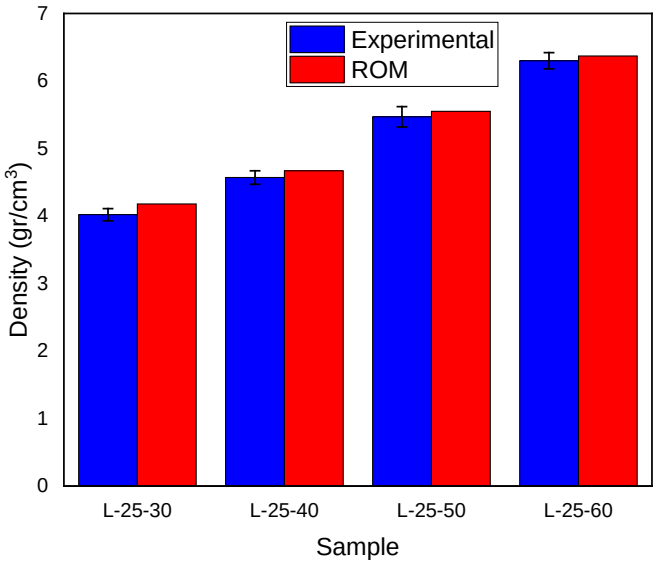

Figure 23: Comparison of the experimental and ROM results of density

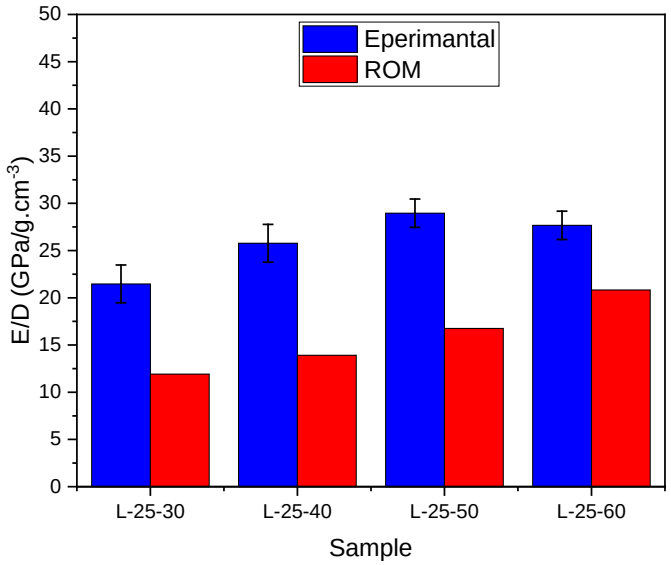

Figure 24: Comparison of the experimental and ROM results of specific stiffness

IV. Conclusions

A comprehensive experimental study was performed to investigate the effect(s) of the core volume fraction and rolling direction on the mechanical properties of the S/P/S composite laminate under uniaxial tensile loading. In the frame of the current study, the following conclusions are made:

1. Due to the higher passing time and consequently the higher effective pressure, the lower rolling speed leads to higher bond strength.
2. By increasing the polymer volume fraction in the laminate structure, the yield behavior becomes the same at RD, DD, and TD. On the other hand, S/P/S Laminates, like monolithic steel sheet exhibit higher ultimate tensile strength at $0°$ and $90°$ orientations, compared to the strength exhibited in a $45°$ orientation. As the volume fraction of the polymer increases, both yield and tensile strengths as well as elastic Young's modulus of laminates decreases.
3. The work hardening exponent (n) of all laminates is almost lower than that of monolithic steel sheet at all directions. Direct correlation between formability and n-value was observed. In other words, similarity of both the value and the trend of results obtained for low carbon steel and S/P/S laminates were indicative of high formability of laminates.
4. Increasing the angular orientation of the tensile samples from $0°$ to $90°$, led too initial increase in the elongation of all laminates. However, the increase was succeeded by decreases in elongation while the skin sheet showed the opposite trend. Moreover high-bond strength laminates have higher elongation than low-bond strength laminates. The difference between the obtained elongations and the calculated ones showed that thicker laminates had a larger volume fraction of micro-cavities that formed after lamination.
5. S/P/S laminates demonstrated homogeneous material behavior. This was the result of consistent stiffness properties in all directions relative to the rolling direction.
6. The likelihood of premature fracture in S/P/S laminates was higher than monolithic steel sheet thanks to occurrence of simultaneous necking of two steel face sheets at the same location.

Conducting experimental and finite element analysis to further understand the effect of interlayer thickness on formability, weldability, and impact resistance of this laminates is essential for improving their properties for various industrial applications. Additionally, the fracture mechanisms of the laminates need to be investigated under various loading conditions.

References Références Referencias

1. A. Carradò, J. Faerber, S. Niemeyer, G. Ziegmann, and H. Palkowski, "Metal/polymer/metal hybrid systems: Towards potential formability applications," *Compos Struct,* vol. 93, no. 2, pp. 715–721, 2011, doi: https://doi.org/10.1016/j.compstruct.2010.07.016
2. M. Damghani, C. Wallis, J. Bakunowicz, and A. Murphy, "Experimental and numerical analysis for postbuckling behaviour of tailored hybrid composite laminates subjected to shear loading," *Compos Struct,* p. Accepted for publication, 2020.

3. M. Damghani, J. Saddler, E. Sammon, G. A. Atkinson, J. Matthews, and A. Murphy, "An experimental investigation of the impact response and Post-impact shear buckling behaviour of hybrid composite laminates," *Compos Struct,* vol. 305, p. 116506, 2023, doi: https://doi.org/10.1016/j.compstruct.2022.116506
4. A. Kwakernaak, J. Hofstede, J. Poulis, and R. Benedictus, "8 - Improvements in bonding metals for aerospace and other applications," in *Woodhead Publishing Series in Welding and Other Joining Technologies,* M. C. B. T.-W. and J. of A. M. Chaturvedi, Ed., Woodhead Publishing, 2012, pp. 235–287. doi: https://doi.org/10.1533/9780857095169.2.235
5. I. Burchitz, R. Boesenkool, S. van der Zwaag, and M. Tassoul, "Highlights of designing with Hylite – a new material concept," *Mater Des,* vol. 26, no. 4, pp. 271–279, 2005, doi: https://doi.org/10.1016/j.matdes.2004.06.021
6. J.-K. Kim and T.-X. Yu, "Forming and failure behaviour of coated, laminated and sandwiched sheet metals: a review," *J Mater Process Technol,* vol. 63, no. 1, pp. 33–42, 1997, doi: https://doi.org/10.1016/S0924-0136(96)02596-4
7. M. Harhash, O. Sokolova, A. Carradó, and H. Palkowski, "Mechanical properties and forming behaviour of laminated steel/polymer sandwich systems with local inlays – Part 1," *Compos Struct,* vol. 118, pp. 112–120, 2014, doi: https://doi.org/10.1016/j.compstruct.2014.07.011
8. J. Liu, W. Liu, and W. Xue, "Forming limit diagram prediction of AA5052/polyethylene/AA5052 sandwich sheets," *Materials & Design (1980-2015),* vol. 46, pp. 112–120, 2013, doi: https://doi.org/10.1016/j.matdes.2012.09.057
9. F. Kazemi, R. Hashemi, and S. A. Niknam, "Formability and fractography of AA5754/polyethylene/AA5754 sandwich composites," *Mechanics Based Design of Structures and Machines,* vol. 50, no. 4, pp. 1253–1267, Apr. 2022, doi: 10.1080/15397734.2020.1747 488
10. K. J. Kim *et al.,* "Formability of AA5182/polypropylene/AA5182 sandwich sheets," *J Mater Process Technol,* vol. 139, no. 1, pp. 1–7, 2003, doi: https://doi.org/10.1016/S0924-0136(03)00173-0
11. K. Logesh and V. K. B. Raja, "Formability analysis for enhancing forming parameters in AA8011/PP/AA1100 sandwich materials," *The International Journal of Advanced Manufacturing Technology,* vol. 93, no. 1, pp. 113–120, 2017, doi: 10.1007/s00170-015-7832-5
12. K. J. Kim *et al.,* "Development of application technique of aluminum sandwich sheets for automotive hood," *International Journal of Precision Engineering and Manufacturing,* vol. 10, no. 4, pp. 71–75, 2009, doi: 10.1007/s12541-009-0073-5
13. V. Satheeshkumar and R. G. Narayanan, "Investigation on the influence of adhesive properties on the formability of adhesive-bonded steel sheets," *Proc Inst Mech Eng C J Mech Eng Sci,* vol. 228, no. 3, pp. 405–425, May 2013, doi: 10.1177/0954406213488727
14. H. Hayashi and T. Nakagawa, "Recent trends in sheet metals and their formability in manufacturing automotive panels," *J Mater Process Technol,* vol. 46, no. 3, pp. 455–487, 1994, doi: https://doi.org/10.1016/0924-0136(94)90128-7
15. J. Liu and L. Zhuang, "Cylindrical cup-drawing characteristics of aluminum-polymer sandwich sheet," *The International Journal of Advanced Manufacturing Technology,* vol. 97, no. 5, pp. 1885–1896, 2018, doi: 10.1007/s00170-018-2077-8
16. M. Nourjani Pourmoghadam, R. Shahrokh Esfahani, M. R. Morovvati, and B. Nekooei Rizi, "Bifurcation analysis of plastic wrinkling formation for anisotropic laminated sheets (AA2024–Polyamide–AA2024)," *Comput Mater Sci,* vol. 77, pp. 35–43, 2013, doi: https://doi.org/10.1016/j.commatsci.2013.03.037
17. M. Harhash, A. Carradó, and H. Palkowski, "DEEP- AND STRETCH-FORMING OF STEEL/POLYMER/STEEL LAMINATES," in *Euro Hybrid Materials and Structures,* Kaiserslautern (Germany), 2016.
18. B. Rezaei Anvar and A. Akbarzadeh, "Roll bonding of AA5052 and polypropylene sheets: Bonding mechanisms, microstructure and mechanical properties," *J Adhes,* vol. 93, no. 7, pp. 550–574, Jun. 2017, doi: 10.1080/00218464.2015.1116067
19. S. Nambu, M. Michiuchi, J. Inoue, and T. Koseki, "Effect of interfacial bonding strength on tensile ductility of multilayered steel composites," *Compos Sci Technol,* vol. 69, no. 11, pp. 1936–1941, 2009, doi: https://doi.org/10.1016/j.compscitech.2009.04.013.
20. H. Park, S.-J. Kim, J. Lee, J. H. Kim, and D. Kim, "Characterization of the Mechanical Properties of a High-Strength Laminated Vibration Damping Steel Sheet and Their Application to Formability Prediction," *Metals and Materials International,* vol. 25, no. 5, pp. 1326–1340, 2019, doi: 10.1007/s12540-019-00281-8
21. R. B. Ruokolainen and D. R. Sigler, "The Effect of Adhesion and Tensile Properties on the Formability of Laminated Steels," *J Mater Eng Perform,* vol. 17, no. 3, pp. 330–339, 2008, doi: 10.1007/s11665-008-9207-7.
22. M. Weiss, B. Rolfe, M. Dingle, and P. Hodgson, "The influence of interlayer thickness and properties on spring-back of SPS- (steel/polymer/steel) laminates.," *Steel grips,* vol. 2, pp. 445–449, 2004, [Online]. Available: https://dro.deakin.edu.au/articles/journal_contribution/The_influence_of_interlayer_thickness_and_properties_on_spring-back_of_SPS-_steel_polymer_steel_laminates_/20537805

23. F. Avril, R. Rahmé, M. Doux, D. Verchere, D. Sage, and P. Cassagnau, "New Polymer Materials for Steel/Polymer/Steel Laminates in Automotive Applications," *Macromol Mater Eng,* vol. 298, no. 6, pp. 644–652, Jun. 2013, doi: https://doi.org/10.1002/mame.201200058
24. T. Saito and N. Mizuhashi, "Resistance welding of vibration-damped steel sheet," *Welding International,* vol. 4, no. 12, pp. 993–997, Jan. 1990, doi: 10.1080/09507119009453040
25. H. Oberle, C. Commaret, C. Minier, R. Magnaud, and G. Pradere, "Optimizing resistance spot welding parameters for vibration damping steel sheets," *Weld J,* vol. 77, 1998, [Online]. Available: https://api.semanticscholar.org/CorpusID:136653269
26. S. Mousa and G.-Y. Kim, "Direct Adhesion of Warm Roll-Bonded Al1100/Polyurethane/Al1100 Sandwich Composite," in *Proceedings of the ASME 2015 International Manufacturing Science and Engineering Conference,* North Carolina (USA), Jun. 2015. doi: 10.1115/MSEC2015-9467
27. W. Lin, X. Li, W. Dong, Y. Zhao, M. Li, and Y. Wang, "Ultrahigh bonding strength and excellent corrosion resistance of Al-TPU hybrid induced by microstructures and silane layer," *J Mater Process Technol,* vol. 296, p. 117180, 2021, doi: https://doi.org/10.1016/j.jmatprotec.2021.117180
28. M. Yahiaoui, J. Denape, J.-Y. Paris, A. G. Ural, N. Alcalá, and F. J. Martínez, "Wear dynamics of a TPU/steel contact under reciprocal sliding," *Wear,* vol. 315, no. 1, pp. 103–114, 2014, doi: https://doi.org/10.1016/j.wear.2014.04.005
29. J. Liu, Q. Zhang, B. Zhang, and M. Yu, "The Influence of the Roll-Laminating Process on the Bonding Quality of Polymer-Coated Steel Interface," *Coatings,* vol. 11, no. 4. 2021. doi: 10.3390/coatings11040472
30. S. Mousa, N. Scheirer, and G.-Y. Kim, "Roll-bonding of metal-polymer-metal sandwich composites reinforced by glass whiskers at the interface," *J Mater Process Technol,* vol. 255, pp. 463–469, 2018, doi: https://doi.org/10.1016/j.jmatprotec.2017.12.039
31. M. Harhash, R. R. Gilbert, S. Hartmann, and H. Palkowski, "Experimental characterization, analytical and numerical investigations of metal/polymer/metal sandwich composites – Part 1: Deep drawing," *Compos Struct,* vol. 202, pp. 1308–1321, 2018, doi: https://doi.org/10.1016/j.compstruct.2018.06.066
32. A. Frick, M. Borm, N. Kaoud, J. Kolodziej, and J. Neudeck, "Microstructure and thermomechanical properties relationship of segmented thermoplastic polyurethane (TPU)," *AIP Conf Proc,* vol. 1593, no. 1, pp. 520–525, May 2014, doi: 10.1063/1.4873835
33. M. Kamali Andani, H. Daneshmanesh, and S. A. Jenabali Jahromi, "Investigation of the bonding strength of the stainless steel 316L/polyurethane/stainless steel 316L tri-layer composite produced by the warm rolling process," *Journal of Sandwich Structures & Materials,* vol. 22, no. 3, pp. 728–742, Apr. 2018, doi: 10.1177/1099636218770911
34. M. Abbasi and M. R. Toroghinejad, "Effects of processing parameters on the bond strength of Cu/Cu roll-bonded strips," *J Mater Process Technol,* vol. 210, no. 3, pp. 560–563, 2010, doi: https://doi.org/10.1016/j.jmatprotec.2009.11.003
35. J. A. DiCello, "Steel-Polypropylene-Steel Laminate – A New Weight Reduction Material," in *1980 Automotive Engineering Congress and Exposition,* SAE International, Feb. 1980. doi: https://doi.org/10.4271/800078
36. A. Forcellese and M. Simoncini, "Mechanical properties and formability of metal–polymer–metal sandwich composites," *The International Journal of Advanced Manufacturing Technology,* vol. 107, no. 7, pp. 3333–3349, 2020, doi: 10.1007/s00170-020-05245-6